Volume 52
Number 37
7 October 2023
Pages 13013-13438

Dalton Transactions

An international journal of inorganic chemistry

rsc.li/dalton

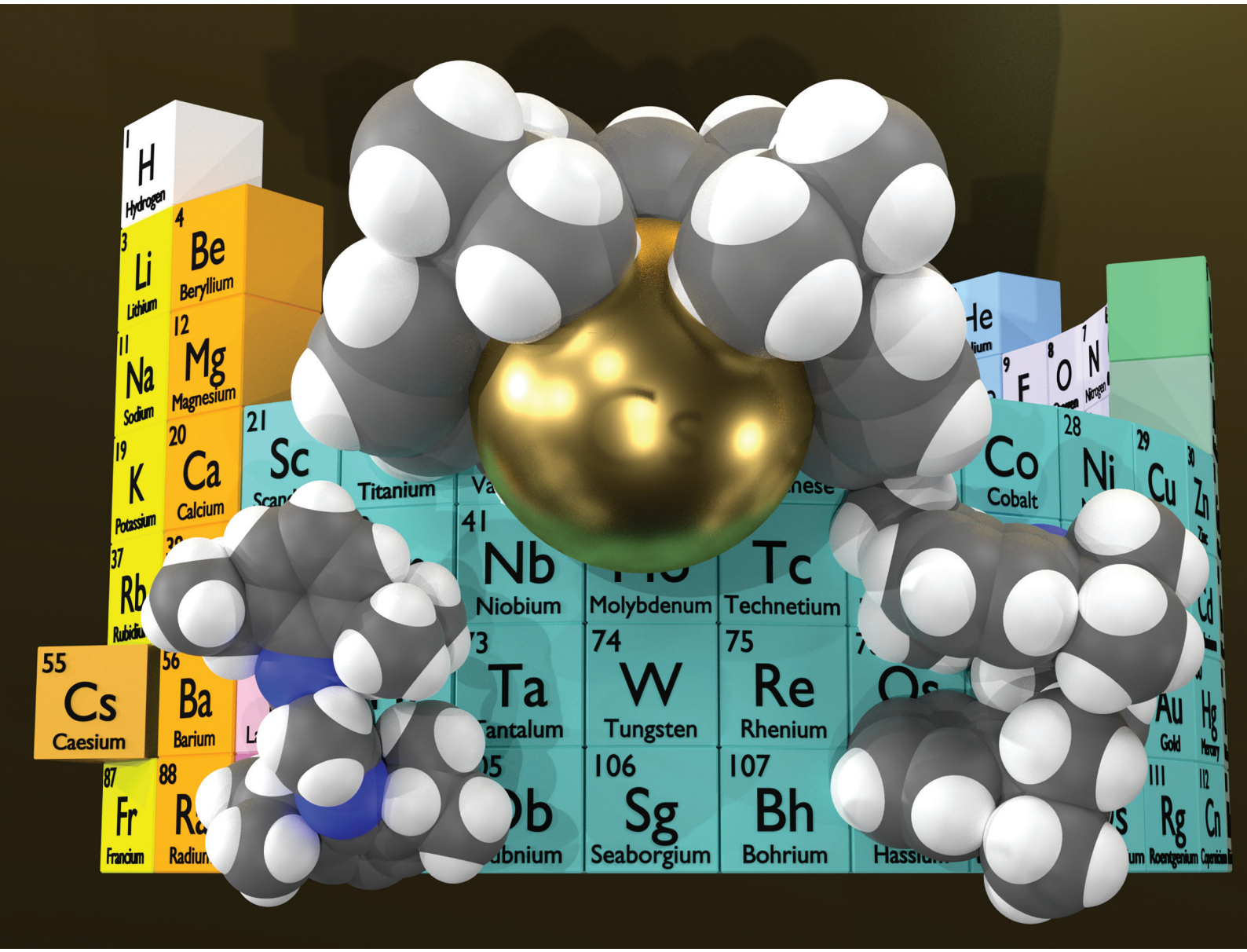

ISSN 1477-9226

ROYAL SOCIETY OF CHEMISTRY

COMMUNICATION

Hellen Videa and Antonio J. Martínez-Martínez

Revealing unbound β-diketiminate anions: structural dynamics from caesium complexes

Dalton Transactions

ROYAL SOCIETY OF CHEMISTRY

COMMUNICATION

View Article Online
View Journal | View Issue

Cite this: *Dalton Trans.*, 2023, **52**, 13058

Received 25th May 2023,
Accepted 15th June 2023

DOI: 10.1039/d3dt01592k

rsc.li/dalton

Revealing unbound β-diketiminate anions: structural dynamics from caesium complexes†‡

Hellen Videa and Antonio J. Martínez-Martínez *

This study reports the first structural elucidation of β-diketiminate anions (BDI$^-$), known for strong coordination, in their unbound form within caesium complexes. β-Diketiminate caesium salts (BDICs) were synthesised, and upon the addition of Lewis donor ligands, free BDI$^-$ anions and donor-solvated Cs$^+$ cations were observed. Notably, the liberated BDI$^-$ anions exhibited an unprecedented dynamic *cisoid–transoid* exchange in solution.

Monoanionic β-diketiminate (BDI) ligands,[1] commonly referred to as NacNac ligands, are an important class of ligands with diverse applications in multiple chemical fields.[2] Characterised by two ketiminate moieties linked by a 1,3-carbon chain, these ligands can be readily obtained *via* the deprotonation of β-diketimines (Fig. 1A).[3] BDI ligands are known for their ability to stabilise a broad array of metal ions from the s,[4] p,[5] d[6] and f-blocks[7] in diverse oxidation states by forming strong coordination complexes. Moreover, they have been shown to enhance catalytic activity, selectivity, and stability in several processes, including olefin polymerisation[8] and copolymerization,[9] transfer hydrogenation,[10] and cross-coupling reactions.[11] BDI ligands have demonstrated potential in developing unique main group species[12] with unconventional electronic and stereochemical properties that enable novel reactivity and catalysis.[13] They have also been used in material science for crafting novel metal–organic frameworks (MOFs),[14] biomedical chemistry for developing new metal-based therapeutics,[15] and biochemistry for modelling metalloenzymes.[16]

While BDI ligands commonly form stable and robust chelating complexes by donating two nitrogen atoms as κ^2-*N*,*N*′-ligands **I** (Fig. 1B),[17] examples of alternative coordination modes involving partial ligand dissociation have also been observed, **II–V**.[18] Recent studies have underscored the importance of the dissociation properties of BDI ligands in catalysis and bond activation chemistry. For instance, BDI dissociation has been shown to boost catalytic activities in lactide polymerisation with (BDI)$_2$ZrCl$_2$ species,[19] trigger C–F activation in hemilabile (BDI)Co(I) complexes,[18d,20] and promote unusual ligand rearrangements during N_2 activation in low-valent [(BDI)Ca(I)]$_2$ species.[21] Thus, understanding the dissociation and free anionic forms of BDI ligands is pivotal for gaining a deeper insight into their chemistry. However, despite their widespread use, examples of free BDI$^-$ anions have remained elusive.

In this study, we explored the free-form structures of BDI$^-$ exhibiting *cisoid–transoid* dynamic behaviour in solution, using various spectroscopic and crystallographic techniques. We report novel examples of unbound ^{Dipp}BDI$^-$ [(DippNCMe)$_2$CH]$^-$ anions (Dipp = 2,6-iPr$_2$C$_6$H$_3$) and examine them in their "*naked*" state, free from metal-ion binding interactions. To achieve this, we selected heavy and soft alkali metal caesium (Cs), the Lewis donor solvent THF, and strongly coordinating secondary ligands such as 18-crown-6 and [2.2.2]

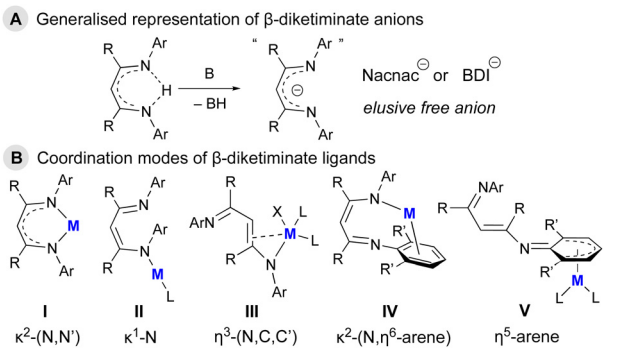

Fig. 1 (A) Generalised representation of β-diketiminate (BDI) anions. (B) Known coordination modes of BDI ligands.

CIQSO – Centre for Research in Sustainable Chemistry and Department of Chemistry, University of Huelva, Campus El Carmen, Huelva ES-21007, Spain. E-mail: antonio.martinez@ciqso.uhu.es

†Dedicated to Professor Robert E. Mulvey for his unwavering guidance and mentorship.

‡Electronic supplementary information (ESI) available: Experimental procedures, characterisation data, selected figures, computational and crystallographic details. CCDC 2256945–2256948. For ESI and crystallographic data in CIF or other electronic format see DOI: https://doi.org/10.1039/d3dt01592k

cryptand. The selection of Cs was motivated by its larger ionic radius and higher polarisability, typically leading to weaker ligand interactions than lighter alkali metals, a behaviour discussed extensively in the context of alkali metal mediation in organometallic chemistry.[22] Our work represents the first identification of BDI^- anions without metal-ion binding, offering valuable insights into their properties.

Deprotonation of the β-diketimine proligand ^{Dipp}BDI(H) by caesium bis(trimethylsilyl)amide CsHMDS[23] occurred quantitatively within 1 h at room temperature (Fig. 2A), as evidenced by ^{1}H NMR spectroscopy. The resulting caesium salt (BDI)Cs was isolated in 45% yield. Crystals of $[(BDI)Cs]_\infty$ **1**, obtained by the slow diffusion of freshly distilled *n*-hexane into a toluene solution of the complex, confirmed the formation of a solvent-free complex (Fig. 2B). The BDI ligand chelates the Cs^+ metal ion (Cs–N 2.972(2) and 2.941(2) Å) in **1**, resembling lighter alkali metal κ^2-*N*,*N*′-derivatives (Li,[24] Na,[25] and K[7d]). Cs coordination is further facilitated by internal Cs···π(η^2-arene) (3.334(2)–3.765(3) Å) contacts, along with additional Cs···π(η^6-arene) (3.35 Å) and Cs···Me (3.828(2) Å) interactions with neighbouring molecules, leading to a zigzag polymeric structure. NMR data of **1**, obtained in Tol-d_8 solution at room temperature, revealed a symmetric C_{2v} BDI skeleton with characteristic resonance signals at δ 4.75 and 1.86 ppm for the backbone γ-CH and Me groups in the ^{1}H NMR spectrum (δ range 4.67–5.10 and 1.75–2.15 ppm, respectively, for Li,[26,24b] Na[25] and K[27]). Diffusion-Ordered NMR Spectroscopy (DOSY) revealed polymer monomerization through the coordination of toluene molecules, leading to $[(BDI)Cs(toluene)_n]$ **1·(toluene)$_n$** monomeric aggregates in Tol-d_8 solution.

When the stronger coordinating solvent THF-d_8 was used, the ^{1}H NMR spectrum of **1** exhibited a noticeable broadening at room temperature. The γ-CH and Me groups resonated as singlets at δ 4.23 and 1.54 ppm, respectively. This suggests that BDI chelates Cs^+, accompanied by further THF coordination. This resulted in monomers identified as $[(BDI)Cs(THF)_n]$ **1·(THF)$_n$**, supported by DOSY NMR studies, resembling the observed behaviour of **1·(toluene)$_n$**. As the temperature decreased, resonance signals of **1·(THF)$_n$** sharpened, with the γ-CH and Me signal appearing at δ 4.21 and 1.52 ppm at 258 K, respectively. Similar to **1·(toluene)$_n$**, the NMR data for **1·(THF)$_n$** in the 333–258 K temperature range reveal a symmetrical BDI array. Interestingly, the ^{1}H NMR spectrum of **1·(THF)$_n$** displayed two additional sets of broad resonances at room temperature, which narrowed into two sets of signals in a 10 : 1 ratio at 258 K (40% relative to that of **1**). Each new set of signals consisted of two distinct Dipp, one γ-CH, and two Me environments, indicating two new asymmetrical BDI species in solution. The significantly shielded γ-CH groups for both species (δ 3.55 ppm, overlapped) suggested discoordination of the BDI ligand (δ 3.80 ppm for γ-CH in related κ^1-(*N*, arene) BDI examples).[18e] Also, the two distinct Me groups resonate at δ 2.51/1.22 and δ 2.16/1.22 for the major and minor BDI species, respectively (note that two Me signals are overlapped), reflecting asymmetric BDI skeletons. We hypothesised that the partial ionisation of **1** in THF-d_8 would lead to the formation of two distinct separated ion pairs (SIPs) of the type $[Cs]^+[BDI]^-$, comprising two types of unbound asymmetrical $[BDI]^-$ anions and free THF-solvated $[(THF)_nCs]^+$ cations. Excitingly, ^{1}H NMR titrations of **1** in THF-d_8 with increasing amounts of the bulkier and strongly coordinating crown ether 18-crown-6 (18-cr-6, 0–2 equiv.) or encapsulating [2.2.2]cryptand (crypt, 0–1 equiv.) exclusively produced these two new asymmetric BDI species in the same ratio as THF-d_8, accompanied by the presence of either $[(18\text{-cr-}6)_2Cs]^+$ or $[(crypt)Cs]^+$ cations. This observation showed, for the first time, the complete dissociation of the BDI ligand, generating SIP species $[(donor)Cs]^+[BDI]^-$ in solution. We attempted kinetic studies to study the pathways and factors governing BDI ligand dissociation; however, our efforts were hindered by the overlapping of NMR signals and the small amount of one of the free BDI^- anionic species in the studied temperature range.

To gain a better understanding of these new BDI species, we synthesised and isolated the corresponding SIP species, $[(18\text{-cr-}6)_2Cs]^+[(BDI)]^-$ **2** and $[(crypt)Cs]^+[(BDI)]^-$ **3** (Fig. 3A). The addition of 18-cr-6 (2 equiv.) and crypt (1 equiv.) to **1** in toluene yielded **2** and **3** as yellow powders in isolated yields of 40 and 54%, respectively. Crystallisation from *n*-hexane/toluene allowed us to obtain crystals of **2a** and **3a**. X-ray diffraction analysis confirmed their arrangements as solvent-separated ion-pairs (Fig. 3B and C). In **2a**, the Cs^+ ion is fully solvated by two molecules of 18-cr-6, whereas in **3a**, Cs^+ is fully entrapped by a crypt molecule. Remarkably, the BDI^- anion remains unbound and adopts a *transoid* conformation (indicated by the relative position of the Me backbone groups). Intriguingly, crystals of a second isomeric form, **2b**, featuring a *ciscoid* conformation of the BDI^- anion, were obtained by crystallising **2** in a mixture of *n*-hexane/THF (Fig. 3C). The metrics

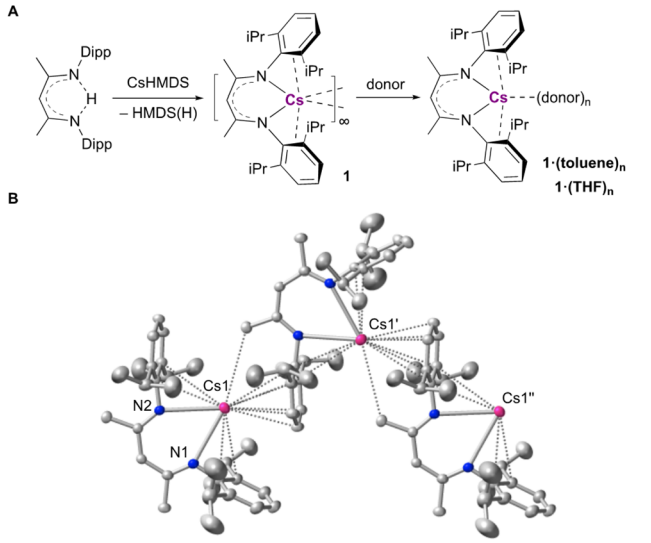

Fig. 2 (A) Synthesis of $[(BDI)Cs]_\infty$ **1**. (B) Crystal structure of **1** showing a section of the polymeric zigzag array *via* Cs···π(arene) and Cs···Me contacts.

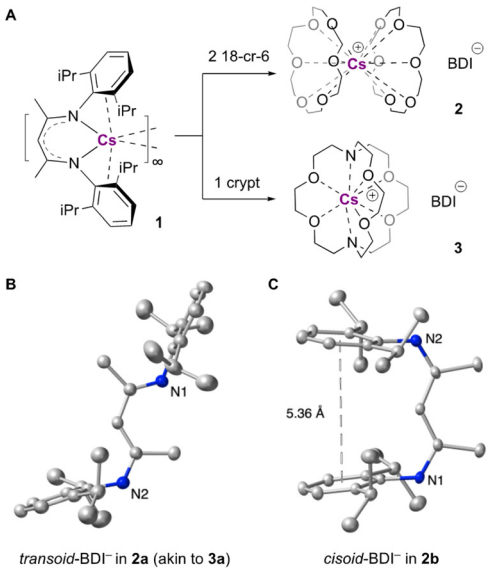

Fig. 3 (A) Synthesis of $[(18\text{-cr-}6)_2Cs]^+[(BDI)]^-$ **2** and $[(crypt)Cs]^+[(BDI)]^-$ **3**. (B) and (C) Crystal structures of **2a** and **2b** showing the *transoid* and *cisoid* isomeric forms of BDI^- anions. **2a** and **3a** exhibit identical *transoid* BDI arrays. The Cs cations were omitted for clarity.

of the cation $[(18\text{-cr-}6)_2Cs]^+$ are similar to those in **2a**. Both the *transoid*-BDI^- and *cisoid*-BDI^- anions in structures **2a**, **2b** and **3a** present average C–N and C–C bond lengths that lie between those of single and double bonds (1.309(4)–1.326(5) and 1.408(4)–1.427(7) Å, respectively), indicative of charge delocalisation across the BDI backbone. A noteworthy feature of **2b** is the BDI^- anions staggered yet eclipsed arrangement of the two aromatic Dipp groups, which are separated by a distance of 5.63 Å.

The reproducibility of multiple independent crystallisations from isolated powders **2** and **3**, yielding *transoid*-BDI^- anions within the structures of **2a** and **3a** and *cisoid*-BDI^- in **2b**, underscores the dynamic nature of free BDI^- anions and their sensitivity to the surrounding environment. This anion sensitivity to environmental conditions is also reflected in the crystal packing effects observed in the structures of **2a**, **2b**, and **3a**. Weak noncovalent $Cs^+\cdots$Me and $Cs^+\cdots\pi$(arene) interactions between the ancillary Dipp aromatic groups of the BDI^- anions and the $[(18\text{-cr-}6)_2Cs]^+$ or $[(crypt)Cs]^+$ cations are evident in structures **2a** and **3a**, where the BDI^- anion adopts a *transoid* arrangement. The absence of these weak interactions in the structure of **2b** promotes a highly compact *cisoid*-BDI^- conformation that compensates for the lack of noncovalent anion–cation interactions. Taken together, these unique BDI^- anion conformations, which are shaped by the presence or absence of weak ionic and noncovalent interactions, highlights the influence of the Cs^+ cations and coordinating ligands on the BDI^- anions.

NMR experiments conducted on small samples of crystals of **2a**, **2b**, and **3a**, or powders **2** and **3**, revealed identical NMR data (^1H and ^{13}C), except for the signals corresponding to the different cations $[(18\text{-cr-}6)_2Cs]^+$ and $[(crypt)Cs]^+$. This finding suggests the rapid interconversion of *cisoid* and *transoid* BDI^- species, following the equilibrium $[(donor)Cs]^+[$*transoid*-$BDI]^-$ ⇄ $[(donor)Cs]^+[$*cisoid*-$BDI]^-$. The absence of any correlation or trend in the ^{133}Cs NMR chemical shifts for the various Cs–BDI complexes indicates that Cs^+ cations are affected by the dynamic nature of the BDI^- anions. Furthermore, 2D chemical exchange ^1H–^1H EXSY NMR experiments on the 18-cr-6 and crypt SIP $[(donor)_nCs]^+[(BDI)]^-$ species confirmed this dynamic process (Fig. 4A), which likely involves bond rotations in the BDI backbone chain. DFT calculations considering THF solvent effects (Fig. 4B) demonstrated that the *transoid* conformation C, characterised in the crystal structures of **2a** and **3a**, is more stable than the *cisoid* conformation E found in **2b**, by 2.6 kcal mol^{-1}. These calculations also suggest that rotations within the BDI^- anion backbone around the C–C and C–N bonds involve almost energetically equivalent *cisoid* and *transoid* rotamers A ⇄ E. Particularly, the unbound chelating conformation A was found to be less stable by 5.2 kcal mol^{-1} when compared to the *transoid* conformation C. Furthermore, DOSY NMR studies support the existence of the SIP species $[(donor)_nCs]^+[(BDI)]^-$, indicating weak noncovalent electrostatic interactions between pairs $[(donor)_nCs]^+\cdots[BDI]^-$. This state suggests high anion polarisation of BDI^- species in solution, requiring electrostatic contact with electropositive $[(donor)_nCs]^+$ cations for stabilisation, similar to the crystal packing effects observed for the *transoid* isomer in the solid-state structures of **2a** and **3a**. Collectively, these findings suggest that the *transoid* arrangement predominates in solu-

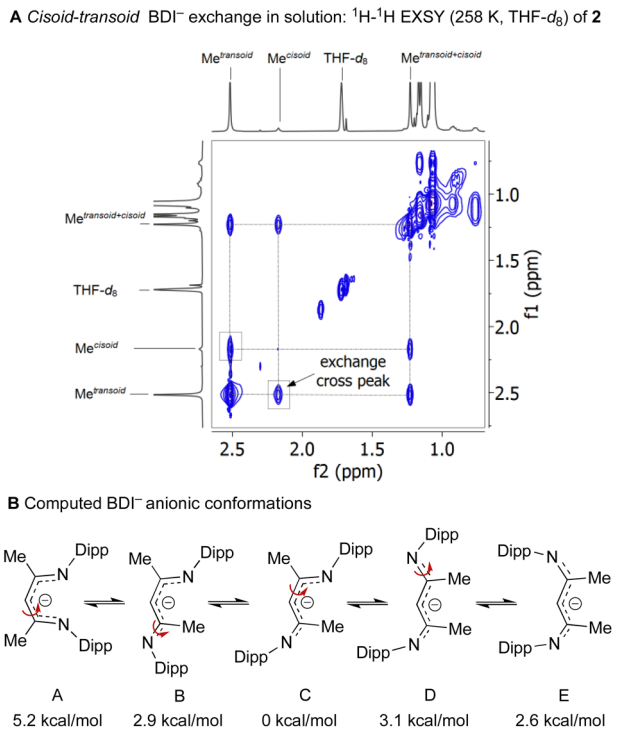

Fig. 4 (A) EXSY NMR study showing *cisoid*–*transoid* exchange between BDI^- anions in **2** in THF-d_8 solution. (B) Conformers of BDI^- anions computed through backbone rotations (Gibbs free energies in THF at 298 K).

tion, emphasising the dynamic behaviour and sensitivity of BDI^- anions to the surrounding ionic environment.

Conclusions

In conclusion, we successfully synthesised and characterised a series of BDI complexes with Cs cations. These complexes dissociate to form solvent-separated ion-pairs with free, unbound BDI^- anions in the presence of coordinating ligands such as THF, 18-cr-6, and crypt. This study provides valuable insights into the structural and dynamic features of unbound BDI^- anions in *cisoid* and *transoid* conformations, and their weak interactions with counterions in solution and in solid form. Notably, the presence of Cs^+ cations enables weak interactions and dynamic *cisoid–transoid* BDI^- exchange in solution, thus challenging the conventional view of BDI ligands as predominantly bound entities to metal ions. These findings have important implications for the design and utilisation of new BDI ligands in coordination chemistry, catalysis, and related areas, encouraging further studies of unbound BDI^- anions within other soft metal systems.

Conflicts of interest

There are no conflicts to declare.

Acknowledgements

The authors acknowledge financial support from the Spanish Ministry of Science and Innovation (PID2019-108292RA-I00, EUR2020-112189), FEDER, the Andalusian Government (P20-00373), the University of Huelva (UHU-202043), and the Spanish Research State Agency AEI for a Ramón y Cajal Research Contract (RYC-2017-21783). We thank Prof. F. J. Blas for his valuable assistance with the computational studies. Funding for open access charge: Universidad de Huelva/CBUA.

References

1 (*a*) S. G. McGeachin, *Can. J. Chem.*, 1968, **46**, 1903–1912; (*b*) J. E. Parks and R. H. Holm, *Inorg. Chem.*, 1968, **7**, 1408–1416.
2 (*a*) L. Bourget-Merle, M. F. Lappert and J. R. Severn, *Chem. Rev.*, 2002, **102**, 3031–3066; (*b*) S. Hohloch, B. M. Kriegel, R. G. Bergman and J. Arnold, *Dalton Trans.*, 2016, **45**, 15725–15745; (*c*) R. L. Webster, *Dalton Trans.*, 2017, **46**, 4483–4498.
3 D. J. Mindiola, P. L. Holland and T. H. Warren, in *Inorg. Synth*, ed. T. B. Rauchfuss, John Wiley & Sons, Inc., 2010, vol. 35, pp. 1–55.
4 S. P. Sarish, S. Nembenna, S. Nagendran and H. W. Roesky, *Acc. Chem. Res.*, 2011, **44**, 157–170.
5 M. Asay, C. Jones and M. Driess, *Chem. Rev.*, 2011, **111**, 354–396.
6 C. Chen, S. M. Bellows and P. L. Holland, *Dalton Trans.*, 2015, **44**, 16654–16670.
7 (*a*) S. V. Klementyeva, M. Y. Afonin, A. S. Bogomyakov, M. T. Gamer, P. W. Roesky and S. N. Konchenko, *Eur. J. Inorg. Chem.*, 2016, **2016**, 3666–3672; (*b*) W. Mao, L. Xiang and Y. Chen, *Coord. Chem. Rev.*, 2017, **346**, 77–90; (*c*) M. A. Boreen, C. A. Gould, C. H. Booth, S. Hohloch and J. Arnold, *Dalton Trans.*, 2020, **49**, 7938–7944; (*d*) O. A. Mironova, T. S. Sukhikh, S. N. Konchenko and N. A. Pushkarevsky, *Inorg. Chem.*, 2022, **61**, 15484–15498.
8 (*a*) D. Liu, C. Yao, R. Wang, M. Wang, Z. Wang, C. Wu, F. Lin, S. Li, X. Wan and D. Cui, *Angew. Chem., Int. Ed.*, 2015, **54**, 5205–5209; (*b*) F. Lin, Z. Liu, M. Wang, B. Liu, S. Li and D. Cui, *Angew. Chem., Int. Ed.*, 2020, **59**, 4324–4328.
9 S.-F. Yuan, Y. Yan, G. A. Solan, Y. Ma and W.-H. Sun, *Coord. Chem. Rev.*, 2020, **411**, 213254.
10 M. Espinal-Viguri, S. E. Neale, N. T. Coles, S. A. Macgregor and R. L. Webster, *J. Am. Chem. Soc.*, 2019, **141**, 572–582.
11 (*a*) A. Bakhoda, O. E. Okoromoba, C. Greene, M. R. Boroujeni, J. A. Bertke and T. H. Warren, *J. Am. Chem. Soc.*, 2020, **142**, 18483–18490; (*b*) R. Li, X. Yang and H. Ping, *Catal. Sci. Technol.*, 2022, **12**, 4281–4287.
12 (*a*) S. P. Green, C. Jones and A. Stasch, *Science*, 2007, **318**, 1754–1757; (*b*) M. Zhong, S. Sinhababu and H. W. Roesky, *Dalton Trans.*, 2020, **49**, 1351–1364; (*c*) C. Färber, P. Stegner, U. Zenneck, C. Knüpfer, G. Bendt, S. Schulz and S. Harder, *Nat. Commun.*, 2022, **13**, 3210.
13 (*a*) M. Arrowsmith, M. S. Hill, G. Kociok-Köhn, D. J. MacDougall and M. F. Mahon, *Angew. Chem., Int. Ed.*, 2012, **51**, 2098–2100; (*b*) T. Chu, I. Korobkov and G. I. Nikonov, *J. Am. Chem. Soc.*, 2014, **136**, 9195–9202; (*c*) M. D. Anker, M. S. Hill, J. P. Lowe and M. F. Mahon, *Angew. Chem., Int. Ed.*, 2015, **54**, 10009–10011; (*d*) L. Davin, R. McLellan, A. R. Kennedy and E. Hevia, *Chem. Commun.*, 2017, **53**, 11650–11653; (*e*) H. Bauer, M. Alonso, C. Färber, H. Elsen, J. Pahl, A. Causero, G. Ballmann, F. De Proft and S. Harder, *Nat. Catal.*, 2018, **1**, 40–47; (*f*) T. N. Hooper, M. Garçon, A. J. P. White and M. R. Crimmin, *Chem. Sci.*, 2018, **9**, 5435–5440; (*g*) M. Magre, B. Maity, A. Falconnet, L. Cavallo and M. Rueping, *Angew. Chem., Int. Ed.*, 2019, **58**, 7025–7029; (*h*) R. M. Gauld, J. R. Lynch, A. R. Kennedy, J. Barker, J. Reid and R. E. Mulvey, *Inorg. Chem.*, 2021, **60**, 6057–6064.
14 N. C. Thacker, Z. Lin, T. Zhang, J. C. Gilhula, C. W. Abney and W. Lin, *J. Am. Chem. Soc.*, 2016, **138**, 3501–3509.
15 J. M. Hope, J. J. Wilson and S. J. Lippard, *Dalton Trans.*, 2013, **42**, 3176–3180.
16 D. J. E. Spencer, N. W. Aboelella, A. M. Reynolds, P. L. Holland and W. B. Tolman, *J. Am. Chem. Soc.*, 2002, **124**, 2108–2109.
17 C. Camp and J. Arnold, *Dalton Trans.*, 2016, **45**, 14462–14498.

18 (*a*) R. J. Wright, P. P. Power, B. L. Scott and J. L. Kiplinger, *Organometallics*, 2004, **23**, 4801–4803; (*b*) W. H. Bernskoetter, E. Lobkovsky and P. J. Chirik, *Organometallics*, 2005, **24**, 6250–6259; (*c*) N. Carrera, N. Savjani, J. Simpson, D. L. Hughes and M. Bochmann, *Dalton Trans.*, 2011, **40**, 1016–1019; (*d*) T. R. Dugan, X. Sun, E. V. Rybak-Akimova, O. Olatunji-Ojo, T. R. Cundari and P. L. Holland, *J. Am. Chem. Soc.*, 2011, **133**, 12418–12421; (*e*) A. J. Wooles, W. Lewis, A. J. Blake and S. T. Liddle, *Organometallics*, 2013, **32**, 5058–5070.

19 (*a*) I. El-Zoghbi, S. Latreche and F. Schaper, *Organometallics*, 2010, **29**, 1551–1559; (*b*) I. El-Zoghbi, T. J. J. Whitehorne and F. Schaper, *Dalton Trans.*, 2013, **42**, 9376–9387.

20 M. H. Al-Afyouni, E. Suturina, S. Pathak, M. Atanasov, E. Bill, D. E. DeRosha, W. W. Brennessel, F. Neese and P. L. Holland, *J. Am. Chem. Soc.*, 2015, **137**, 10689–10699.

21 B. Rösch, T. X. Gentner, J. Langer, C. Färber, J. Eyselein, L. Zhao, C. Ding, G. Frenking and S. Harder, *Science*, 2021, **371**, 1125–1128.

22 T. X. Gentner and R. E. Mulvey, *Angew. Chem., Int. Ed.*, 2021, **60**, 9247–9262.

23 A. I. Ojeda-Amador, A. J. Martínez-Martínez, A. R. Kennedy and C. T. O'Hara, *Inorg. Chem.*, 2016, **55**, 5719–5728.

24 (*a*) B. A. Jazdzewski, P. L. Holland, M. Pink, V. G. Young, D. J. E. Spencer and W. B. Tolman, *Inorg. Chem.*, 2001, **40**, 6097–6107; (*b*) M. Stender, R. J. Wright, B. E. Eichler, J. Prust, M. M. Olmstead, H. W. Roesky and P. P. Power, *J. Chem. Soc., Dalton Trans.*, 2001, 3465–3469; (*c*) N. Burford, M. D'Eon, P. J. Ragogna, R. McDonald and M. J. Ferguson, *Inorg. Chem.*, 2004, **43**, 734–738; (*d*) P. Jutzi, K. Leszczyńska, A. Mix, B. Neumann, W. W. Schoeller and H.-G. Stammler, *Organometallics*, 2009, **28**, 1985–1987; (*e*) R. M. Gauld, J. R. Lynch, A. R. Kennedy, J. Barker, J. Reid and R. E. Mulvey, *Inorg. Chem.*, 2021, **60**, 6057–6064.

25 B. Rösch, T. X. Gentner, J. Eyselein, J. Langer, H. Elsen and S. Harder, *Nature*, 2021, **592**, 717–721.

26 B. Qian, D. L. Ward and M. R. Smith, *Organometallics*, 1998, **17**, 3070–3076.

27 W. Clegg, E. K. Cope, A. J. Edwards and F. S. Mair, *Inorg. Chem.*, 1998, **37**, 2317–2319.